Composites Science and Technology 242 (2023) 110169

Contents lists available at ScienceDirect

Composites Science and Technology

journal homepage: www.elsevier.com/locate/compscitech

Multiple-stimuli response composite hydrogels with high mechanical property and triple shape memory effect

Qiangwang Geng [a], Fenghua Zhang [a], Yanju Liu [b], Jinsong Leng [a,*]

[a] Centre for Composite Materials and Structures, Harbin Institute of Technology (HIT), Harbin, 150080, People's Republic of China
[b] Department of Astronautical Science and Mechanics, Harbin Institute of Technology (HIT), Harbin, 150001, People's Republic of China

ARTICLE INFO

Handling Editor: Dr. Ming-Qiu Zhang

Keywords:
Shape memory hydrogel
Gelatin/PAAm/A11AUA
Near infrared
Composite hydrogel

ABSTRACT

Shape memory hydrogels are widely used in soft robots and other fields. However, it is difficult to realize multiple-shape memory hydrogels with high strength and simple driving modes. The mechanical properties of a hydrogel were improved in this study through the creation of a double network hydrogel using a combination of gelatin and PAAm. Additionally, hydrogen bonding was introduced into the structure of the hydrogel through the incorporation of acryl 11-aminodecanoic acid (A11AUA). The helical structure of gelatin and the semi-crystalline segment of A11AUA provide enabling the hydrogels to realize a triple shape memory effect at different temperatures. In addition, we found that the hydrogel could also complete shape memory behavior in the $FeCl_3$ solution due to the carboxyl group in A11AUA. And we prepared composite hydrogel to realize remote infrared driving by introducing nano Fe_3O_4. We believe that this triple-shape memory hydrogel with high mechanical property and multiple stimulus responses can expand the application of hydrogel in soft robots, sensors, and other fields.

Author statement

Qiangwang Geng: Conceptualization, Methodology, Investigation, Writing–Original Draft, Writing–Review & Editing, Formal Analysis. Fenghua Zhang: Conceptualization, Supervision, Writing–Review & Editing. Yanju Liu: Formal analysis, Writing–Review & Editing. Jinsong Leng: Conceptualization, Resources, Writing–Review & Editing.

1. Introduction

With the rapid developments of technology as well as incremental social production needs in numerous sectors, soft robotics has been widely introduced and studied due to its sensitivity and special applications under certain extreme conditions [1–4]. However, the adoption of soft robots to a large extent, is considerably limited by their mechanical properties that the soft robot can only carry on certain simple mechanical movements [5,6]. In this regard, studying and applying the shape memory function of soft materials with high mechanical property may contribute to achieving more human-like robot behavior. Deformation of materials can allow them to reach their destination in small volumes resulting in terrific flexibility, and then restore to their original shape to fulfill their functions [7–10]. Therefore, the exploration of shape-memory materials holds great potential in the research of soft robotics.

Shape-memory hydrogels (SMHs) are smart materials that could change their shape under certain external conditions such as influences of heat, light (UV; near-infrared), pH, and others [11–14]. Its shape memory mechanism tends to be achieved through reversible covalent or non-covalent chemical bonds, for instance, hydrogen bonding, dipole-dipole interaction, hydrophobic association, coordination bond and host guest interaction [15–18]. Due to the flexible shape changes and easily achievable external conditions required for its shape transformation, SMHs have been extensively applied in biological actuators, sensors, biomedical devices as well as in soft robots [19–22].

As of today, there are many investigations and reports regarding SMHs. Most of the researches focused on deformation under the control of temperature or pH, whereas, little research has been done on programmable shape-memory hydrogels [23,24]. Appropriately exploiting programmable shape-memory hydrogels may significantly expand the mechanical flexibility of the soft robot, leading to better simulations of the human body [25,26]. Hence, the research on programmable shape-memory hydrogels is indispensable and should draw more

* Corresponding author.
E-mail address: lengjs@hit.edu.cn (J. Leng).

https://doi.org/10.1016/j.compscitech.2023.110169
Received 9 May 2023; Received in revised form 8 July 2023; Accepted 16 July 2023
Available online 20 July 2023

attention from researchers. Previous studies on programmable shape-memory hydrogels have typically relied on the use of multiple external stimuli [27–31]. This approach has been applied to a variety of shape-memory hydrogel applications. For instance, Lu et al. proposed a new double-layer hydrogel with a thermal responsive driving layer and a metal ion responsive memory layer. And the desirable function of the programmable shape memory effect was realized through the combined influences of temperature and calcium ions [32]. It is worth knowing that the preparation process is very complicated and it is quite difficult to fulfill the function of the shape memory effect by using a variety of external stimuli in practice. Thus, it is essential to find an approach to drive the programmable shape-memory hydrogel under alternative and easy-to-implement external conditions.

Shape memory composite materials can effectively solve the above problems. S. Leungpuangkaew et al. developed multi-stimuli-responsive SMPs from bio-based benzoxazine resin and iron oxide nanoparticles (Fe_3O_4 NPs) that could be actuated by magnetic field and light [33,34]. Recently, Zhang's group developed a programmable shape-memory hydrogel by facilitating the reactivity of calcium ions to the blank glucuronic acid in the alginate group of the i-PAP hydrogel (PAAm/alginate-PBA). Nevertheless, due to its poor mechanical property, its applications have been severely limited [35]. So, it is worthwhile to propose a method to solve the mentioned above problems, namely, to prepare a programmable shape-memory hydrogel with the better mechanical property.

In this work, we prepared a programmable shape-memory hydrogel with high mechanical property in the adoption of a simple method. The A11AUA was synthesized according to the previous method [36]. Furthermore, we introduced the A11AUA into the gelatin/PAAm double network system. The triple shape memory effect of hydrogels under thermally independent conditions was achieved through the helical structure of gelatin and semi-crystalline segment of A11AUA. The mechanical property of hydrogels was improved by exerting double network structures and hydrogen bonds. As there are carboxyl groups in the material system, we found that it could also conduct shape memory behavior under the action of Fe^{3+} solution. To facilitate the applications of shape-memory hydrogels, we prepared a composite hydrogel by introducing nano Fe_3O_4 to the hydrogels which could be driven remotely under near-infrared light. We believe that this work will provide new research ideas contributing to the development in the field of deformable robots or sensors in the coming future.

2. Experimental sections

2.1. Materials

Gelatin, *N*, *N*′-Methylenebisacrylamide (MBA), 11-Aminoundecanoic acid, nanometer ferric oxide and Acrylamide (AAm, 99%) were provided by Aladdin (Shanghai) Inc. Acryloyl chloride was obtained from Seans (Tianjin) Inc. hydrochloric acid, sodium hydroxide, tetrahydrofuran (anhydrous) potassium peroxydisulfate (KPS) , Ethyl acetate and petroleum ether were all provided by Tianjin Jiayu Fine Chemical Co., Ltd. All reagents were used as received without the need for further purification.

2.2. Synthesis of A11AUA

To obtain A11AUA, a method previously reported in the literature was employed. Briefly, 0.1 mol NaOH and 0.067 mol 11-Aminoundecanoic acid were weighed into a 250 ml three-necked flask. Following this, 150 ml of deionized water was added to the mixture and the resulting solution was heated to 40 °C while stirring until all other substances were fully dissolved. The solution was then ready for further processing. Under the condition of an ice-water bath, a mixture of 8 ml acryloyl chloride and 10 ml tetrahydrofuran was added dropwise. After allowing the reaction to proceed for 24 h, the resulting product was treated by adjusting its pH to 3. Extraction in ethyl acetate took the supernatant liquid and rotated it. Then we added petroleum ether to reverse the precipitation of white material, afterwards, extracted the filter, and dried the product, which was A11AUA. Fig. S1 depicts the infrared spectra (FTIR) and nuclear magnetic resonance spectrometry (^{1}H-NMR) of the A11AUA, providing valuable information about its chemical structure and composition.

Table 1
The material composition of G-A hydrogel.

Composites	Gelatin (wt %)	AAm (wt %)	MBAA (wt %)	KPS (wt %)	H_2O (wt %)
G5-A	5	11	0.05	0.23	84
G10-A	10	11	0.05	0.23	79
G15-A	15	11	0.05	0.23	74
G20-A	20	11	0.05	0.23	69
G15-A10	15	10	0.05	0.23	75
G15-A15	15	15	0.05	0.23	70
G15-A20	15	20	0.05	0.23	65
G15-A25	15	25	0.05	0.23	60
G15-A30	15	30	0.05	0.23	55

2.3. Fabrication of Gelatin/PAAm (G-A) hydrogel

The synthesis of G-A hydrogels was carried out by a one-pot method adopting thermal curing. First of all, G-A hydrogels with different proportions of gelatin were synthesized, and gelatin with 5%, 10%, 15%, and 20% mass fractions was added respectively whilst keeping the mass fraction of AAm unvaried. A proper amount of MBA, deionized water, and KPS were added to the system, and cured at 60 °C for 1 h, and then placed at 0 °C for 30 min. Afterwards, to maintain the mass fraction of gelatin unchanged, 15% gelatin was chosen due to its superior mechanical properties and shape memory characteristics. Different proportions of acrylamide were then added individually. An appropriate amount of MBA, deionized water, and KPS were utilized in the system and cured at 60 °C for 1 h, and then placed at 0 °C for 30 min. Table 1 shows the material composition of G-A hydrogel.

2.4. Fabrication of gelatin/PAAm/A11AUA (G-A-A) hydrogel

The synthesis of G-A-A hydrogels was also performed by a one-pot method using thermal curing. We chose the G-A hydrogel with the best ratio of gelatin and AAm above and added different proportions of A11AUA (the ratio of A11AUA to AAm). Next, put an appropriate amount of NaOH, MBA, and heated to 60 °C and stirred until completely dissolved. Subsequently, after the solution was lowered to room temperature, an appropriate amount of KPS was added. And it was further transferred to the prepared mold and cured at 80 °C for 1 h. Then placed at 0 °C for 30 min. Table 2 shows the material composition of G-A-A hydrogel.

2.5. Fabrication of gelatin/PAAm/A11AUA-Fe_3O_4(G-A-A-Fe_3O_4) hydrogel

According to the above experiments, we selected the optimal proportion, added the appropriate amount of AAm, gelatin, A11AUA, NaOH, and MBA into the beaker, heated the compound to 60 °C, and stirred until completely dissolved. Then, after lowering the solution to room temperature, added different content of Fe_3O_4 (0.2%–1.0%), and placed in the ultrasonic instrument for 20 min to make Fe_3O_4 disperse evenly, and then KPS was added. Next to this, we transferred the mixture to the prepared mold, cured it at 80 °C for 1 h, and then placed it at 0 °C for 30 min.

Table 2
The material composition of G-A-A hydrogel.

Composites	Gelatin (wt%)	AAm (wt%)	A11AUA (wt%)	NaOH (wt%)	MBAA (wt%)	KPS (wt%)	H_2O (wt%)
G-A-0.5 A	15	20	0.5	0.005	0.05	0.23	64.2
G-A-1.0 A	15	20	1	0.01	0.05	0.23	63.7
G-A-1.5 A	15	20	1.5	0.015	0.05	0.23	63.5
G-A-2.0 A	15	20	2	0.02	0.05	0.23	62.7
G-A-2.5 A	15	20	2.5	0.025	0.05	0.23	62.2

2.6. Characterization

2.6.1. Shape memory behavior

The shape-memory behavior of G-A-A hydrogels was investigated by measuring the thermal changes of hydrogels at different temperatures using DSC/700 of Mettler-Toledo, Switzerland by heating from 0 °C to 150 °C at the rate of 5 °C/min. And the prepared G-A-A hydrogels were cut into long strips (20 mm × 4 mm × 2 mm). To verify its programmable shape memory performance, the dynamic mechanical analysis (DMA, TA Instruments Q800) was engaged to test its glass transition temperature by heating from 0 °C to 90 °C at the rate of 5 °C/min. To verify the crystallinity of the hydrogel, an XRD instrument (Rigaku D/Max 2500) coupled with Cu Kα radiation (λ = 0.154 nm) was used to detect the prepared G-A-A hydrogel. To test the programmable shape memory behavior of the hydrogel, the hydrogel was first deformed at a high temperature and subsequently placed at a low temperature to observe if it recovers. Tests of the programmable shape memory effect of the G-A-A hydrogels under different temperatures were then performed. The shape I was given at a high temperature, shape II was given at a low temperature, and then both of these were heated up to observe their shape return. We also tested the shape memory effect of the G-A hydrogel for comparison. Plenty of experiments were executed to quantitatively calculate the shape fixation rate (R_f) and recovery rate (R_r) according to the Equation (1) and Equation (2) of the G-A, G-A-A, and G-A-A-Fe_3O_4 hydrogels [37].

$$R_f = \frac{180 - \theta_f}{180} \times 100\% \quad (1)$$

$$R_r = \frac{\theta_r - \theta_f}{180 - \theta_f} \times 100\% \quad (2)$$

Where the θ_f is the temporarily fixed angle, and θ_r is the final angle.

2.6.2. Mechanical properties

The prepared G-A-A hydrogels were sliced into elongated strips (length: 20 mm, width: 4 mm, thickness: 0.15 mm). Subsequently,

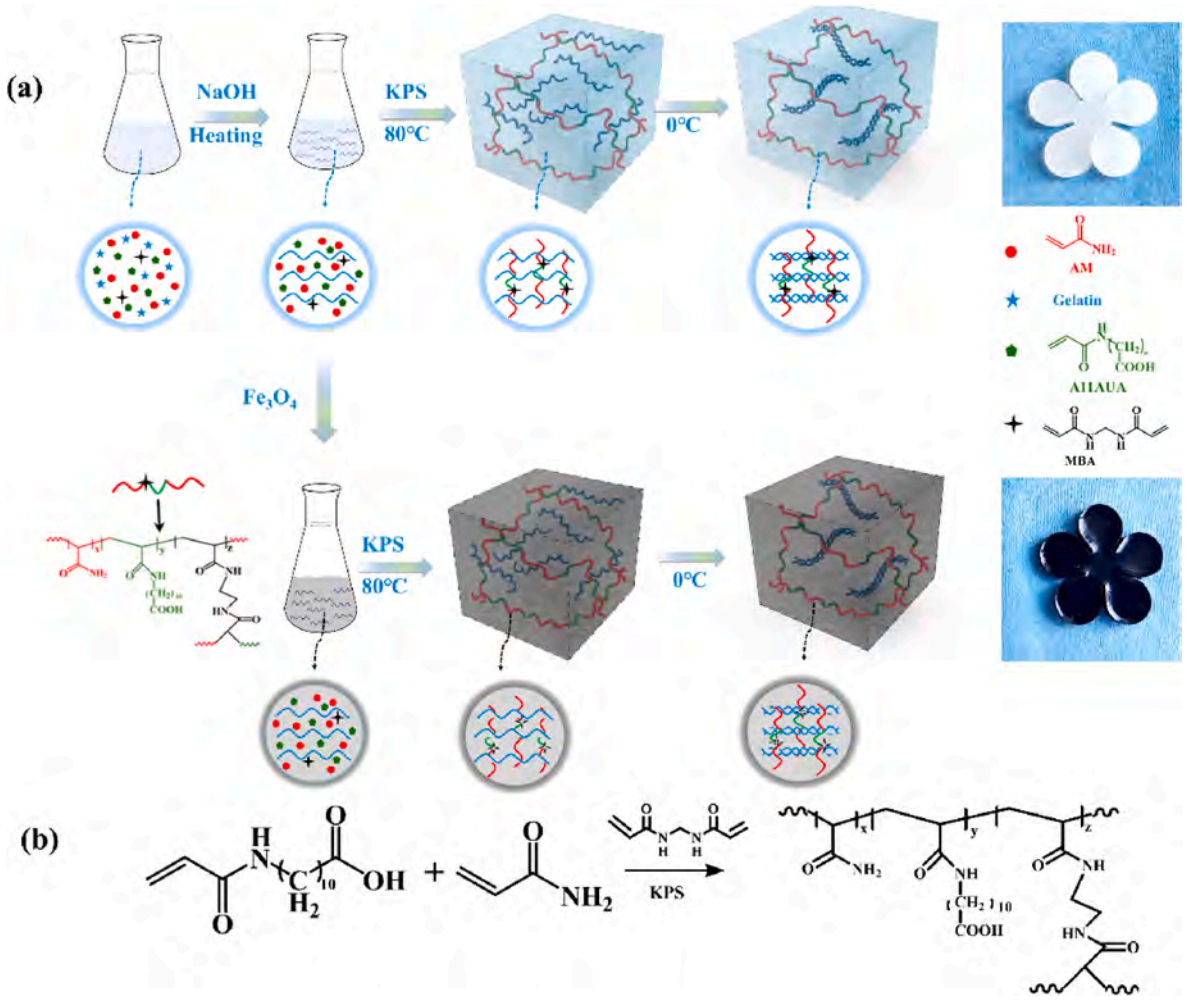

Fig. 1. (a) The synthesis process of G-A-A and G-A-A-Fe_3O_4 hydrogels. (b) Crosslinking diagram of AAm and A11AUA.

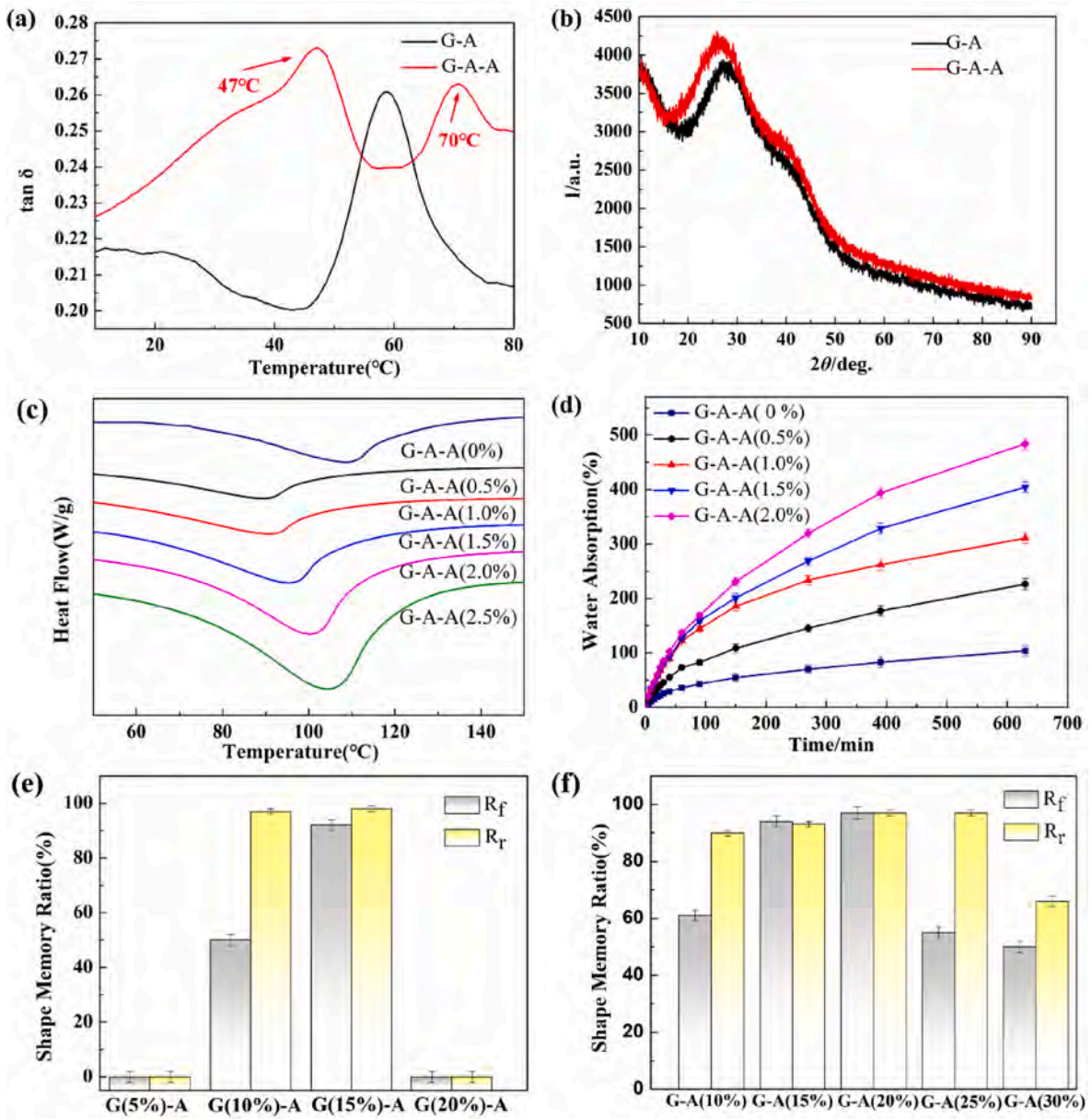

Fig. 2. (a) DMA curves of G-A and G-A-A hydrogels. (b) XRD curves of G-A and G-A-A hydrogels. (c) DSC curves of G-A-A hydrogels. (d) Swelling properties of G-A-A hydrogels. (e)R_f and R_r of G_X-A hydrogels. (f) R_f and R_r of G-A_X hydrogels.

stress-strain curves were generated by conducting mechanical tests on the samples using an electromechanical universal testing machine (CMT2103) at room temperature.

2.6.3. Swelling behavior

The swelling test of hydrogels was carried out by placing the G-A-A and the G-A-A-Fe_3O_4 hydrogels in deionized water and taking them out every other time to measure their mass at room temperature. To determine the swelling ratio (SR), the calculation was performed using Equation (3). The W_1 is the mass after immersion, and W_0 is the initial mass:

$$SR = (W_1 – W_0)/W_0 \times 100\% \quad (3)$$

2.6.4. Morphology

To observe the internal structure of the hydrogel, we freeze-dried the G-A-A-Fe_3O_4 hydrogels and sampled gold spray to observe its internal pore structure through a scanning electron microscope (SEM).

3. Results and discussion

Fig. 1(a) illustrates the straightforward synthesis process of the G-A-A hydrogel. Firstly, gelatin, AAm, A11AUA, MBA, and NaOH were dissolved in deionized water under the condition of heating. At this point, the gelatin network was formed. Then, under the thermal initiator KPS, heating up to 80 °C, AAm and A11AUA were cross-linked under the action of MBA to form a second network which is shown in Fig. 1(b). Eventually, the hydrogel prepared above was placed at 0 °C for 30 min, and the gelatin network composed a helical structure. Furthermore, if moderate nano Fe_3O_4 was added before adding KPS, G-A-A-Fe_3O_4 hydrogels would be synthesized. By testing the infrared spectrum of G-A and G-A-A hydrogels, the enhancement of the infrared characteristic peak of the amide group (1550 cm^{-1} which showed in Fig. S2) proved that A11AUA was successfully introduced into the G-A hydrogel system.

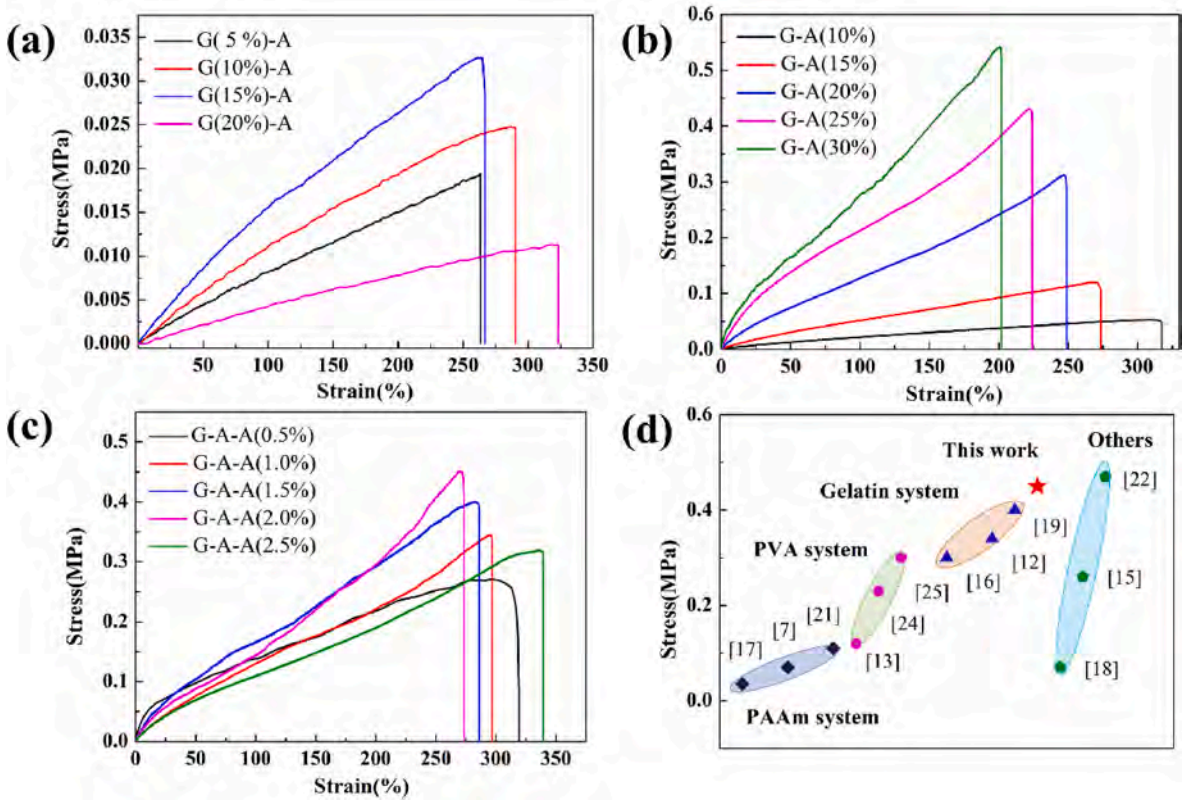

Fig. 3. (a) Stress-strain curves of G-A hydrogels with various gelatin content. (b) Stress-strain curves of G-A hydrogels with various acrylamide content. (c) Stress-strain curves of G-A-A hydrogels with various A11AUA content. (d) Comparison of mechanical.

3.1. Shape memory behavior

To test the shape memory performance of the G-A and G-A-A hydrogels, we first performed DMA tests whose results are shown in Fig. 2(a). And it is apparent that the G-A-A hydrogel has two peaks: at 47 °C and 70 °C while the G-A hydrogel has only one peak at 57 °C. It is caused by the spiral-like structure of gelatin and the crystallization of A11AUA. Since the system has two peaks which are also far apart, we speculate that the G-A-A hydrogel could perform triple-shape memory behavior. The curve of the modulus of G-A-A hydrogel changing with temperature is shown in Fig. S3. Fig. 2(b) shows the XRD curves of G-A and G-A-A hydrogels. The G-A-A hydrogel shows a broad peak at $2\theta = 25.6°$, which is related to the crystallization of alkyl chains in the A11AUA structure. In addition, we tested the DSC curves of G-A-A hydrogels with different proportions of A11AUA shown in Fig. 2(c). It is noticeable that as the A11AUA content rises, the crystalline melting peaks of the G-A-A hydrogels gradually increase and the initial melting temperature of crystallization is about 65 °C. Fig. 2(d) shows the swelling properties of the G-A and G-A-A hydrogels, it is obviously observable that the swelling rate of G-A-A hydrogels grows with the increase of A11AUA content, which might be related to the introduction of the hydrogen bond.

To rule out the effects of the swelling of the G-A-A hydrogel on its triple-shape memory behavior, we did the following tests which are shown in Fig. S4. The G-A-A hydrogel with the initial shape was placed in water at 45 °C for 20 s, applying an external force to give it a temporary shape. After shaping, the G-A-A hydrogel was immersed in water at room temperature to examine the impact of swelling on its shape memory properties. It could be seen that the G-A-A hydrogel with the temporary shape still maintained its temporary shape after 2 h. After two days it basically reverted to the initial shape of the G-A-A hydrogel.

In order to explore the influence of different material contents on shape memory properties, we conducted the shape memory tests on the G-A hydrogels and calculated their R_f and R_r according to Equation (1) and Equation (2).

We conduct shape memory tests by changing the gelatin content of the G-A hydrogels (Fig. S5). And the 15% gelatin content had the best shape memory performance which showed the highest R_f and R_r (Fig. 2 (e)). Subsequently, we fixed the proportion of gelatin to 15%, changed the proportion of acrylamide, and tested its shape memory performance. With the increase of acrylamide content, its shape memory performance became stronger, but an excessive amount of acrylamide would reduce its shape memory performance (Fig. S6). By calculating R_f and R_r, it showed that 20% acrylamide had the best shape memory performance (Fig. 2(f)). With the increase of acrylamide content, the crosslinking degree of acrylamide increases, limiting the changes in the structure of gelatin. Therefore, its shape memory performance will decrease.

3.2. Mechanical properties

Fig. 3(a) is a stress-strain curve of the G-A hydrogel with constant content of acrylamide engaging in changing the content of gelatin. When the gelatin content is 15%, the mechanical properties of G-A hydrogel are the strongest, with 0.034 MPa. We kept the gelatin content constant at 15%, added different proportions of acrylamide, and tested its stress-strain curve as shown in Fig. 3(b). With the increased content of acrylamide, the mechanical strength of G-A hydrogel rises, but its elongation at break falls. Considering the shape memory property of G-A hydrogel, we chose the G-A hydrogel with 20% acrylamide whose mechanical property is 0.31 MPa.

After determining the optimal raw material content of G-A hydrogel, we added A11AUA in different proportions. Their stress-strain curves are shown in Fig. 3(c). It can be observed that the mechanical strength of G-A-A hydrogel increases with the addition of A11AUA but decreases with the content of A11AUA of 2.5%. The maximum value is 0.45 MPa with the content of A11AUA of 2%. This might be attributable to the

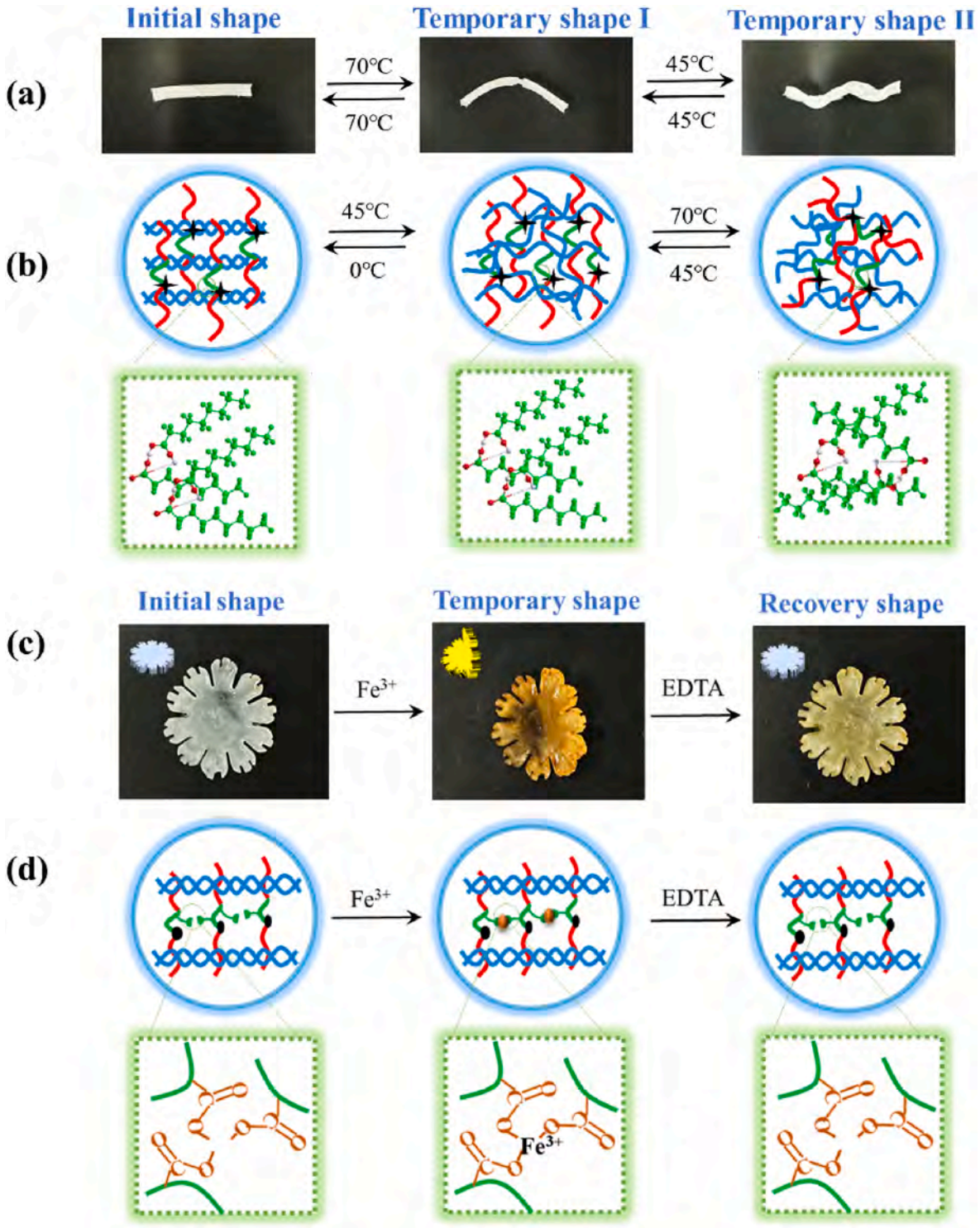

Fig. 4. (a) Programmable shape memory performances of G-A-A hydrogel. (b) Deformation mechanism of G-A-A hydrogel and crystallization change of A11AUA. (c) The G-A-A hydrogel was fixed in $FeCl_3$ and recovered in EDTA solution. (d) Deformation mechanism of G-A-A hydrogel.

addition of A11AUA, which increased the hydrogen bond formed by the acrylamide system. However, more A11AUA needs more NaOH solution to dissolve. More NaOH may react with carboxyl groups, resulting in a decrease in hydrogen bonding and a decrease in its mechanical properties. When the A11AUA content is 2.5%, its mechanical properties decrease. The introduction of A11AUA not only introduced the triple shape memory effect but also enhanced the mechanical properties of hydrogels. So, 2% content of A11AUA was chosen as the optimal ratio and carried out the following shape memory behavior tests.

In Fig. 3(d), a comparison is made between the mechanical properties of the G-A-A hydrogel and those of other shape memory hydrogels. It is worth noting that these hydrogels are with similar water content. The results indicate that, in general, shape memory hydrogels exhibit mechanical properties below 0.3 MPa, whereas our research has achieved a value of 0.45 MPa. This demonstrates that the G-A-A hydrogel has superior mechanical property.

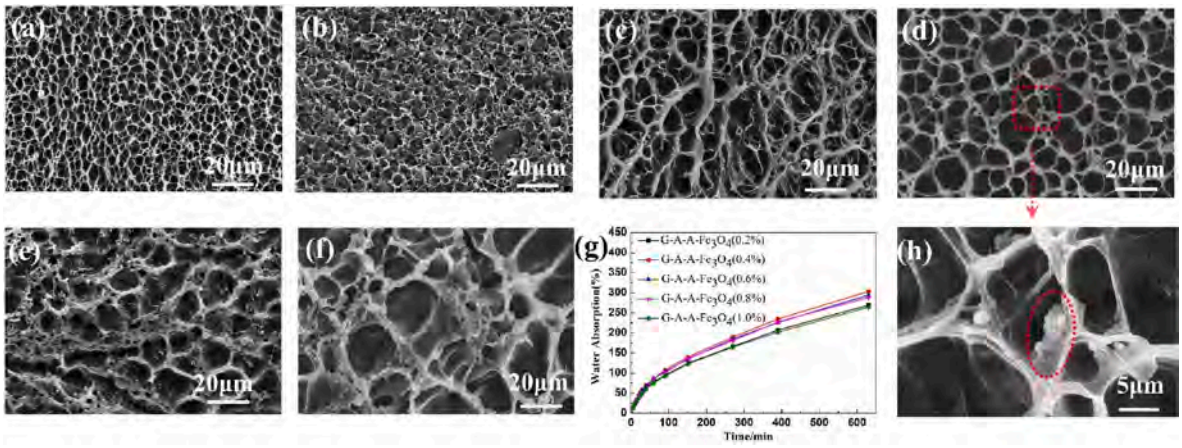

Fig. 5. (a)–(f) Microstructure of G-A-A-Fe_3O_4 hydrogels with the content from 0%,0.2%,0.4%,0.6%,0.8%,1.0% of the Fe_3O_4. (g) The swelling properties of G-A-A-Fe_3O_4 hydrogels. (h) Nano Fe_3O_4 in the G-A-A-Fe_3O_4 hydrogel.

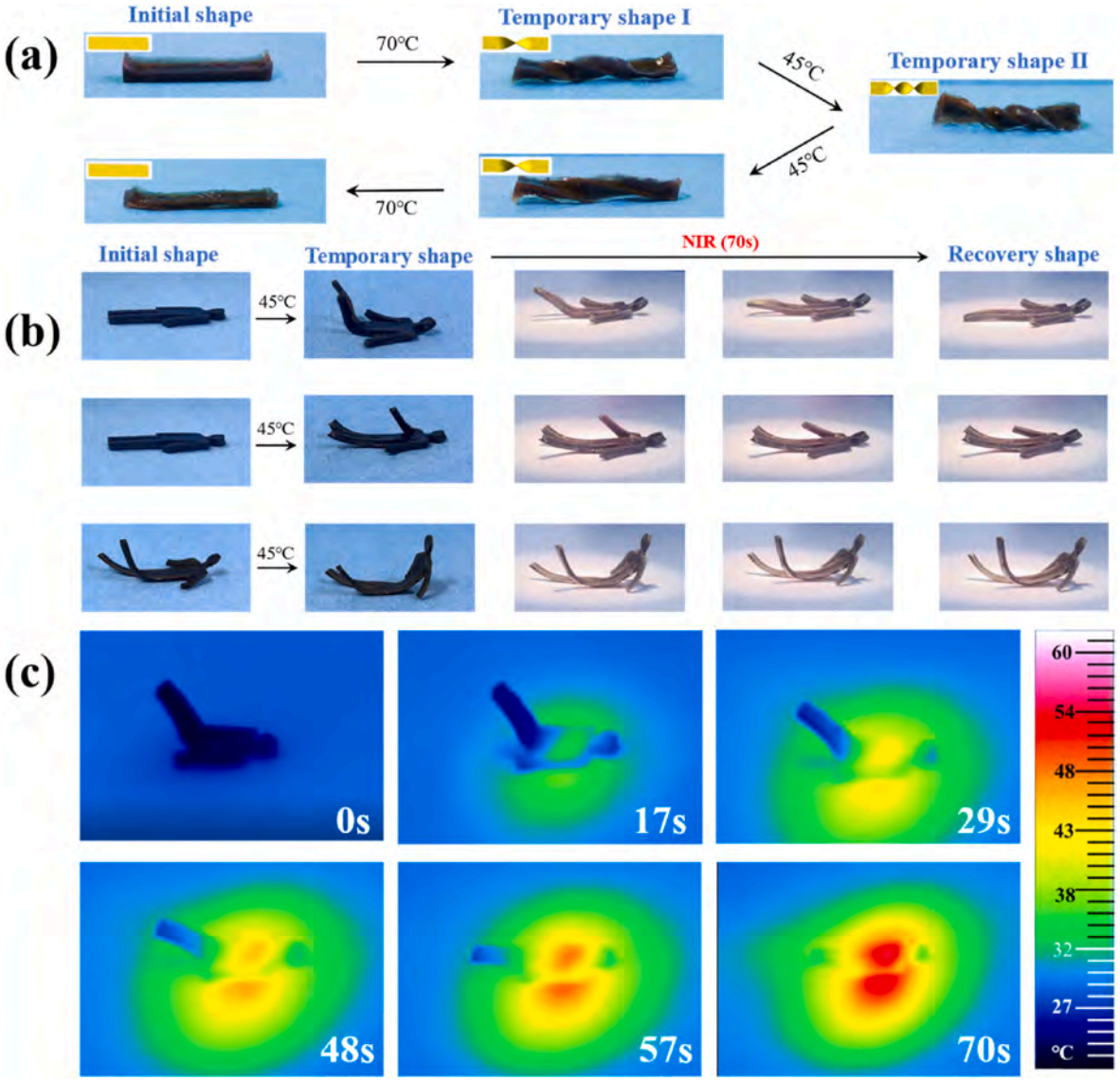

Fig. 6. (a) Programmable shape memory performances of G-A-A-Fe_3O_4 hydrogel. (b) Near-infrared driving shape memory performances of G-A-A-Fe_3O_4 hydrogel. (c) The temperature change of the G-A-A-Fe_3O_4 hydrogel under NIR irradiation.

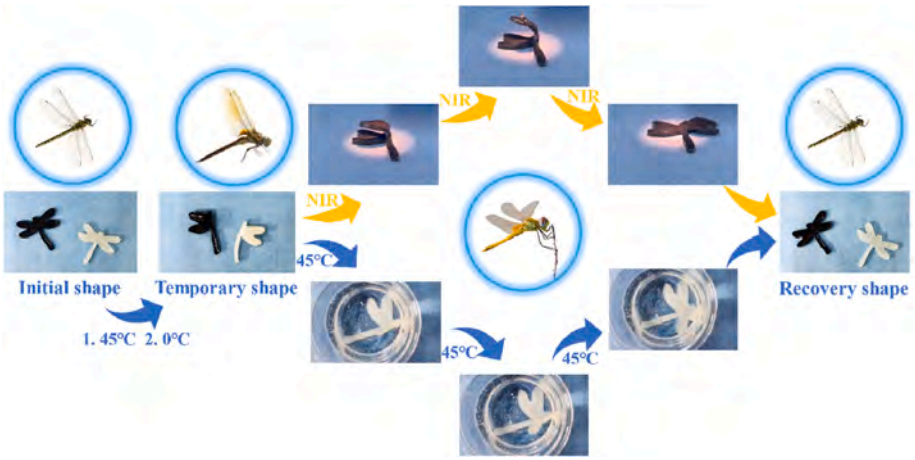

Fig. 7. Shape memory performances of bionic dragonfly hydrogels.

3.3. Shape memory performance of G-A-A hydrogels

Fig. 4 shows the triple-shape memory behavior of G-A-A hydrogels. First, the initial shape of G-A-A hydrogel was soaked in water at 70 °C for 20 s, and an external force was applied to give it a temporary shape I. Then it was placed at 0 °C, and gelatin was transformed into the helicoid structure. The G-A-A hydrogel with the temporary shape I was then soaked in water at 45 °C for 20 s, it was clearly found that it could maintain the shape of temporary I. Then an external force was applied, giving the G-A-A hydrogel a temporary shape II. And place it at 0 °C to maintain its shape. Upon immersing the G-A-A hydrogel with temporary shape II in water at 45 °C for 20 s, it was found that the hydrogel could be restored to the shape of temporary shape I, as illustrated in Fig. 4(a). Similarly, when the G-A-A hydrogel with the temporary shape I was subjected to water at 70 °C for 20 s, it returned to its original shape. These results are quite remarkable and highlight the impressive shape memory properties of the G-A-A hydrogel. This fast and programmable shape memory behavior of this G-A-A hydrogel expands the application of shape memory hydrogels.

Fig. 4(b) depicts the mechanism of the impressive shape memory performance of the G-A-A hydrogels. The helical structure of gelatin provides the hydrogels with remarkable shape memory properties at low temperatures. Moreover, the semi-crystalline segments of A11AUA allow the hydrogel to exhibit shape memory behavior at higher temperatures.

Because A11AUA introduced carboxyl groups into the hydrogel system, we tested the G-A-A hydrogel shape memory performance in the $FeCl_3$ solution. The temporary shape of the G-A-A hydrogel was fixed in $FeCl_3$ solution and its shape was restored in EDTA solution (Fig. 4(c)). The carboxylic acids in A11AUA and gelatin form metal coordination bonds with Fe^{3+} ions, enabling a response to metal ions which showed in Fig. 4(d). This boosts the ability of the G-A-A hydrogel to deform in multiple dimensions. In addition, we tested the R_f of different A11AUA contents in $FeCl_3$ solution and Rr in EDTA (Fig. S7). We found that with the rise of the A11AUA content of the G-A-A hydrogel, its R_f and R_r increased (Fig. S8). However, its R_f could only reach 80%, which might be associated with the low content of A11AUA.

3.4. Microstructure of G-A-A-Fe_3O_4 hydrogels

To facilitate the use of the G-A-A hydrogels in practical applications, we added nano ferric oxide particles to enable the G-A-A hydrogel to drive shape memory behavior remotely.

Fig. 5(a–f) shows the microstructure of the G-A-A-Fe_3O_4 hydrogels which are freeze-dried with different contents of nano Fe_3O_4 through SEM. As it can be seen from Fig. 5(a–f), as the nano Fe_3O_4 content increases, the size of the hole of the G-A-A-Fe_3O_4 hydrogel becomes larger. This could be due to nano Fe_3O_4 occupying some space inside the G-A-A hydrogel. We also measured the swelling of the G-A-A-Fe_3O_4 hydrogel shown in Fig. 5 (g). Its swelling ratio is not changed much, but compared with the hydrogel without nanoparticles (Fig. 2(d)), its swelling ratio is greatly reduced, from 484% to 300% after immersing in the water for 10 h. Fig. 5 (h) clearly shows nano Fe_3O_4 in the G-A-A-Fe_3O_4 hydrogel. And the distribution of Fe elements was showed in Fig. S9.

3.5. Shape memory performance of G-A-A-Fe_3O_4 hydrogels

We first verified the programmable shape memory effect of G-A-A-Fe_3O_4 hydrogels (Fig. 6 (a)). Obviously, it can be observed that the G-A-A-Fe_3O_4 hydrogel can still be programmed for the shape memory effect. We prepared three groups of hydrogel humans to verify their shape memory effect (Fig. 6 (b)). First, the hydrogel humans were heated to 45 °C and applied external force to lift their legs, and arms and make them sit up. They were then placed at 0 °C to have their shape fixed. After that, placed under an 808 nm infrared light and observed their shape recovery effect. It was found that they could return to their original shape under infrared driving (Movie S1-3). The Shape memory performance was tested of the G-A-A-Fe_3O_4 with the different content of nano Fe_3O_4 (Fig. S10). With the increase of the content of nano Fe_3O_4, the recovery time decreased. When the content of nano Fe_3O_4 is 1%, the recovery time is in the 70s (Fig. S11). To investigate the near-infrared response mechanism of G-A-A-Fe_3O_4 hydrogel, we conducted tests on its temperature variation under infrared irradiation shown in Fig. 6 (c). We observed that with increasing irradiation time, the temperature gradually increased, reaching the deformation temperature of the hydrogel.

Supplementary video related to this article can be found at https://doi.org/10.1016/j.compscitech.2023.110169

This mechanism is attributed to the photothermal conversion performance of magnetite nanoparticles (Fe_3O_4) present in the hydrogel.

The G-A-A hydrogels and G-A-A-Fe_3O_4 hydrogels were made in the form of a bionic dragonfly and simulated the unfolding process of its wings through shape memory performances shown in Fig. 7. Firstly, the hydrogels were given temporary shapes i.e., the dragonfly wings, then put them together at 45 °C, and then placed them at 0 °C to maintain the temporary shape. Afterwards, the hydrogels with temporary shape were placed under the 808 nm near-infrared lamp to observe their shape recovery process. The G-A-A-Fe_3O_4 hydrogel restored its shape i.e., the dragonfly wings, and expanded within 100s (Movie S4) while the G-A-A hydrogel couldn't restore its shape (Movie S5). Therefore, it was verified that the photothermal effect produced by nano Fe_3O_4 induces the G-A-A-

Fe_3O_4 hydrogel complete shape recovery. And the G-A-A hydrogel was put in 45 °C water and found that it could quickly restore its shape i.e., the dragonfly wings and expanded (Movie S6). We simulated the spreading process of dragonfly wings under the stimulation of near-infrared and warm water.

Supplementary video related to this article can be found at https://doi.org/10.1016/j.compscitech.2023.110169

4. Conclusion

In conclusion, we prepared a triple shape memory effect hydrogel with excellent mechanical property which could reach 0.45 MPa. Its shape memory effect is achieved through the helical structure of gelatin and the crystallization of A11AUA. The triple shape memory behavior can be fulfilled at 45 °C and 70 °C. The composite hydrogel was prepared by introducing nano ferric oxide, which can achieve remote recovery under near-infrared. The hydrogel humans and bionic dragonfly soft robots were constructed, and their shape memory behavior of infrared response was demonstrated. We believe that this new triple shape memory hydrogel can be widely used in various intelligent fields.

Declaration of competing interest

The authors declare that they have no known competing financial interests or personal relationships that could have appeared to influence the work reported in this paper.

Data availability

Data will be made available on request.

Acknowledgments

Thanks to the National Key R&D Program of China (2022YFB3805700).

Appendix A. Supplementary data

Supplementary data to this article can be found online at https://doi.org/10.1016/j.compscitech.2023.110169.

References

[1] G.M. Whitesides, Soft robotics, Angew. Chem. Int. Ed. 57 (16) (2018) 4258–4273, https://doi.org/10.1002/anie.201800907.
[2] W. Heng, S. Solomon, W. Gao, Flexible electronics and devices as human–machine interfaces for medical robotics, Adv. Mater. 34 (16) (2022), 2107902, https://doi.org/10.1002/adma.202107902.
[3] S. Qi, H.Y. Guo, J. F, Y.P. Xie, M. Zhu, M. Yu, 3D printed shape-programmable magneto-active soft matter for biomimetic applications, Compos. Sci. Technol. 188 (2020), 107973, https://doi.org/10.1016/j.compscitech.2019.107973.
[4] D.C. Zhang, J.W. Zhang, Y.K. Jian, B.Y. Wu, H.Z. Yan, H.H. Lu, S.X. Wei, S. Wu, Q. J. Xue, T. Chen, Multi-field synergy manipulating soft polymeric hydrogel transformers, Adv. Intell. Sist. 3 (4) (2021), 2000208, https://doi.org/10.1002/aisy.202000208.
[5] A. Baranwal, P.K. Agnihotri, Harnessing fiber induced anisotropy in design and fabrication of soft actuator with simultaneous bending and twisting actuations, Compos. Sci. Technol. 230 (2022), 109724, https://doi.org/10.1016/j.compscitech.2022.109724.
[6] S. Qi, J. Fu, Y. Xie, Y. Li, R. Gan, M. Yu, Versatile magnetorheological plastomer with 3D printability, switchable mechanics, shape memory, and self-healing capacity, Compos. Sci. Technol. 183 (2019), 107817, https://doi.org/10.1016/j.compscitech.2019.107817.
[7] F. Zhang, L. Xiong, Y. Ai, Z. Liang, Q. Liang, Stretchable multi responsive hydrogel with actuatable, shape memory, and self-healing properties, Adv. Sci. 5 (8) (2018), 1800450, https://doi.org/10.1002/advs.201800450.
[8] L. Xu, J. Zhao, M. Shi, J. Liu, Z. Wang, Thermodynamic properties of TPI shape memory polymer composites reinforced by GO/SiO_2 modified carbon fiber, Compos. Sci. Technol. 226 (2022), 109551, https://doi.org/10.1016/j.compscitech.2022.109551.
[9] S. Yang, Y. He, J.S. Leng, Shape memory poly (ether ether ketone) s with tunable chain stiffness, mechanical strength and high transition temperatures, Int. J. Smart Nano Mater. 13 (1) (2022) 1–16, https://doi.org/10.1080/19475411.2022.2053228.
[10] J. Hu, N. Jiang, J. Du, Thermally controlled large deformation in temperature-sensitive hydrogels bilayers, Int. J. Smart Nano Mater. 12 (4) (2021) 450–471, https://doi.org/10.1080/19475411.2021.1958091.
[11] Y.Q. Wang, Y. Zhu, J.H. Wang, X.N. Li, X.G. Wu, Y.X. Qin, W.Y. Chen, Fe3+, NIR light and thermal responsive triple network composite hydrogel with multi-shape memory effect, Compos. Sci. Technol. 206 (2021), 108653, https://doi.org/10.1016/j.compscitech.2021.108653.
[12] B. Lv, X. Bu, Y. Da, P. Duan, H. Wang, J. Ren, B. Lyu, D. Gao, J. Ma, Gelatin/PAM double network hydrogels with super-compressibility, Polymer 210 (2020), 123021, https://doi.org/10.1016/j.polymer.2020.123021.
[13] X. Le, W. Lu, J. Zheng, D. Tong, N. Zhao, C. Ma, H. Xiao, J. Zhang, Y. Huang, T. Chen, Stretchable supramolecular hydrogels with triple shape memory effect, Chem. Sci. 7 (11) (2016) 6715–6720, https://doi.org/10.1039/c6sc02354a.
[14] J. Tang, T. Xing, J. Feng, Dual encryption in a shape memory hydrogel with rewritable fluorescent information, Adv. Mater. Technol. (2023), 2201624, https://doi.org/10.1002/admt.202201624.
[15] T. Koga, K. Tomimori, N. Higashi, Transparent, high-strength, and shape memory hydrogels from thermo-responsive amino acid–derived vinyl polymer networks, Macromol. Rapid Commun. 41 (7) (2020), 1900650, https://doi.org/10.1002/marc.201900650.
[16] R.Z. Alavijeh, P. Shokrollahi, J. Barzin, A thermally and water activated shape memory gelatin physical hydrogel, with a gel point above the physiological temperature, for biomedical applications, J. Mater. Chem. B 5 (12) (2017) 2302–2314, https://doi.org/10.1039/c7tb00014f.
[17] G. Li, T. Gao, G. Fan, Z. Liu, Z. Liu, Ji. Jiang, Y. Zhao, Photo-responsive shape memory hydrogels for complex deformation and solvent-driven actuation, ACS Appl. Mater. Interfaces 12 (5) (2019) 6407–6418, https://doi.org/10.1021/acsami.9b19380.
[18] L. Lu, T. Tian, S. Wu, T. Xiang, S. Zhou, A pH-induced self-healable shape memory hydrogel with metal coordination cross-links, Polym. Chem. 10 (15) (2019) 1920–1929, https://doi.org/10.1039/C9PY00015A.
[19] J. Huang, L. Zhao, T. Wang, W.X. Sun, Z. Tong, NIR-triggered rapid shape memory PAM–GO–gelatin hydrogels with high mechanical strength, ACS Appl. Mater. Interfaces 8 (19) (2016) 12384–12392, https://doi.org/10.1021/acsami.6b00867.
[20] Y.Q. Li, X. Xie, Q.X. Zhu, S.R. Lua, Y.K. Bai, A novel smart composite: from self-powered sensors to multi-responsive shape memory actuators, J. Mater. Chem. 10 (41) (2022) 22205–22213, https://doi.org/10.1039/D2TA06626B.
[21] X. Duan, J. Yu, Y. Zhu, Z. Zheng, Q. Liao, Y. Xiao, Y. Li, Z. He, Y. Zhao, H. Wang, L. Qu, Large-scale spinning approach to engineering knittable hydrogel fiber for soft robots, ACS Nano 14 (11) (2020) 14929–14938, https://doi.org/10.1021/acsnano.0c04382.
[22] K. Liu, Y. Zhang, H. Cao, H. Liu, Y. Geng, W. Yuan, J. Zhou, Z. Wu, G. Shan, Y. Bao, Q. Zhao, T. Xie, P. Pan, Programmable reversible shape transformation of hydrogels based on transient structural anisotropy, Adv. Mater. 32 (28) (2020), 2001693, https://doi.org/10.1002/adma.202001693.
[23] X. Zhang, J.Q. Cai, W.Q. Liu, W.F. Liu, X.Q. Qiu, Synthesis of strong and highly stretchable, electrically conductive hydrogel with multiple stimuli responsive shape memory behavior, Polymer 188 (2020), 122147, https://doi.org/10.1016/j.polymer.2019.122147.
[24] M. Guo, J. Yan, X. Yang, J. Lai, P. An, Y.P. Wu, Z.Y. Li, W. Lei, A.T. Smithd, L. Sun, A transparent glycerol-hydrogel with stimuli-responsive actuation induced unexpectedly at subzero temperatures, J. Mater. Chem. B 9 (12) (2021) 7935–7945, https://doi.org/10.1039/D1TA00112D.
[25] D. Zhang, J. Zhang, Y. Jian, B. Wu, H. Yan, H. Lu, S. Wei, S. Wu, Q. Xue, T. Chen, Multi-field synergy manipulating soft polymeric hydrogel transformers, Adv. Intell. Syst. 3 (4) (2021), 2000208, https://doi.org/10.1002/aisy.202000208.
[26] H. Lu, B. Wu, X. Le, W. Lu, Q. Yang, Q. Liu, J. Zhang, T. Chen, Programming shape memory hydrogel to a pre-encoded static deformation toward hierarchical morphological information encryption, Adv. Funct. Mater. 32 (45) (2022), 2206912, https://doi.org/10.1002/adfm.202206912.
[27] G. Fan, S. Wang, Y. Zhang, Z. Liu, Z. Liu, L. Wang, J. Jiang, G. Li, Programmable thermo-responsive actuation of hydrogels via light-guided surface growth of active layers on shape memory substrates, Macromol. Rapid Commun. 44 (4) (2023), 2200705, https://doi.org/10.1002/marc.202200705.
[28] X. Le, W. Lu, H. Xiao, L. Wang, Fe^{3+}-, pH, thermo-responsive supramolecular hydrogel with multi-shape memory effect, ACS Appl. Mater. Interfaces 9 (10) (2017) 9038–9044, https://doi.org/10.1021/acsami.7b00169.
[29] M.N.I. Shiblee, K. Ahmed, M. Kawakami, H. Furukawa, 4D printing of shape-memory hydrogels for soft-robotic functions, Adv. Mater. Technol. 4 (8) (2019), 1900071, https://doi.org/10.1002/admt.201900071.
[30] Q. Wang, L. Zhu, D. Wei, H. Sun, C. Tang, Z. Liu, K. Li, J. Yang, G. Qin, G. Sun, Q. Chen, Near-infrared responsive shape memory hydrogels with programmable and complex shape-morphing, Sci. China Technol. Sci. 64 (8) (2021) 1752–1764, https://doi.org/10.1007/s11431-020-1735-9.
[31] W. Zhao, Z.P. Huang, L.W. Liu, W.B. Wang, J.S. Leng, Y.J. Liu, Porous bone tissue scaffold concept based on shape memory PLA/Fe_3O_4, Compos. Sci. Technol. 203 (2021), 108563, https://doi.org/10.1016/j.compscitech.2020.108563.
[32] H. Lu, B. Wu, X. Yang, J. Zhang, Y. Jian, H. Yan, D. Zhang, Q. Xue, T. Chen, Actuating supramolecular shape memorized hydrogel toward programmable shape deformation, Small 16 (48) (2020), 2005461, https://doi.org/10.1002/smll.202005461.
[33] S. Leungpuangkaew, L. Amornkitbamrung, N. Phetnoi, C. Sapcharoenkun, C. Jubsilp, S. Ekgasit, S. Rimdusit, Magnetic-and light-responsive shape memory polymer nanocomposites from bio-based benzoxazine resin and iron oxide

nanoparticles, Adv. Ind. Eng. Polym. Res. (2023), https://doi.org/10.1016/j.aiepr.2023.01.003.

[34] P. Mora, C. Jubsilp, C.H. Ahn, S. Rimdusit, Two-way thermo-responsive thermoset shape memory polymer based on benzoxazine/urethane alloys using as self-folding structures, Adv. Ind. Eng. Polym. Res. 6 (1) (2023) 13–23, https://doi.org/10.1016/j.aiepr.2022.09.001.

[35] F. Zhang, L. Xiong, Y. Ai, Z. Liang, Q. Liang, Stretchable multi responsive hydrogel with actuatable, shape memory, and self-healing properties, Adv. Sci. 5 (8) (2018), 1800450, https://doi.org/10.1002/advs.201800450.

[36] Q. Geng, C. Zhang, K. Zheng, J. Zhang, J. Cheng, W. Yang, Preparation and properties of a self-healing, multiresponsive color-change hydrogel, Ind. Eng. Chem. Res. 59 (22) (2020) 10689–10696, https://doi.org/10.1021/acs.iecr.0c00219.

[37] F. Zhang, L. Wang, Z. Zheng, Y. Liu, J.S. Leng, Magnetic programming of 4D printed shape memory composite structures, Compos. Part A Appl. Sci. Manuf. (2019), 105571, https://doi.org/10.1016/j.compositesa.2019.105571.